ACS ES&T Water

pubs.acs.org/estwater

Article

Temporal Dynamics of Cyanobacterial Bloom Community Composition and Toxin Production from Urban Lakes

Julie A. Maurer,[⊥] Runjie Xia,[⊥] Andrew M. Kim, Nana Oblie, Sierra Hefferan, Hannuo Xie, Angela Slitt, Bethany D. Jenkins, and Matthew J. Bertin*

Cite This: *ACS EST Water* 2024, 4, 3423−3432

Read Online

ACCESS | Metrics & More | Article Recommendations | Supporting Information

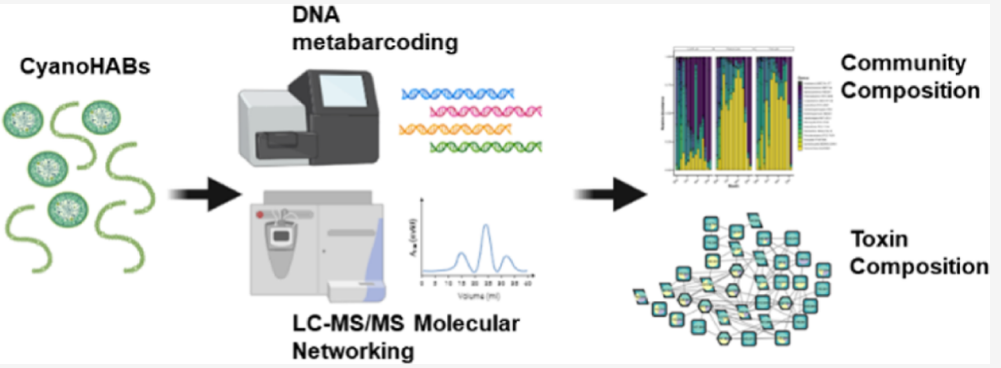

ABSTRACT: With a long evolutionary history and a need to adapt to a changing environment, cyanobacteria in freshwater systems use specialized metabolites for communication, defense, and physiological processes. Furthermore, many cyanobacterial specialized metabolites and toxins present significant human health concerns due to their liver toxicity and their potential impact to drinking water. Gaps in knowledge exist with respect to changes in species diversity and toxin production during a cyanobacterial bloom (cyanoHAB) event; addressing these gaps will improve understanding of impacts to public and ecological health. In the current report we detail community and toxin composition dynamics during a late bloom period. Species diversity decreased at all study sites over the course of the bloom event, and toxin production reached a maximum at the midpoint of the event. We also isolated three new microcystins from a *Microcystis* dominated bloom (**1**−**3**), two of which contained unusual doubly homologated tyrosine residues (**1** and **2**). This work provokes intriguing questions with respect to the use of allelopathy by organisms in these systems and the presence of emerging toxic compounds that can impact public health.

KEYWORDS: *cyanobacteria, harmful algal blooms, microcystins, molecular networking, DNA, metabarcoding*

1. INTRODUCTION

Cyanobacterial blooms (cyanoHABs) are complex microbial systems subject to alterations in abiotic and biotic parameters. These blooms produce a suite of alkaloidal neurotoxins and peptidic hepatotoxins, which can cause nonalcoholic fatty liver disease and acute liver failure.[1,2] Additionally, these events pose significant risks to fresh drinking water resources, perhaps most vividly exemplified by the Toledo Water Crisis of 2014, in which levels of the hepatotoxic microcystin-LR (MC-LR) in drinking water led to a "do not drink; do not use" warning.[3] The majority of research and environmental monitoring has been devoted to microcystin-LR, and concentration limits are set by the US EPA (1.6 μg/L = do not drink; 20 μg/L = do not use). The World Health Organization only sets exposure guidelines for this one microcystin variant (MC-LR) and three alkaloidal toxins (anatoxin-a, saxitoxin, and cylindrospermopsin).[4] However, over 2400 cyanobacterial metabolites have been described to date, including over 300 microcystins along with other cyanopeptides such as the anabaenopeptins, cyanopeptolins, and microginins.[5]

Understanding the full suite of toxins and the temporal resolution of their production is key to determining the full human health impact of these events and the impact of these metabolites on shaping bacterial communities. CyanoHABs represent a complex mixture of species and toxins. Many species in these events have different toxin biosynthesis capabilities, and the toxins produced vary in potency and biological mechanism of action.[6] Water monitoring and treatment can only account for toxins that are currently

Received: March 28, 2024
Revised: July 11, 2024
Accepted: July 12, 2024
Published: July 18, 2024

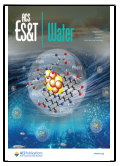

https://doi.org/10.1021/acsestwater.4c00266
ACS EST Water 2024, 4, 3423−3432

known, and many testing methods are not able to distinguish between microcystin congeners of varying potency. These additional toxins (AKA emerging cyanobacterial toxins, ECTs) would not be monitored in raw water, treated water, or finished water. Our group and collaborators have previously used a large-scale harvesting platform to access unprecedented amounts of cyanobacteria biomass, leading to chemical extraction, fractionation, metabolite profiling, and isolation procedures. This research enabled the identification of new exquisitely potent cytotoxic metabolites (the cyanobufalins) and new potently cytotoxic microcystins (MCs).[7,8]

The cyanobacterial communities in these systems change due to nitrogen source (nitrogen fixers vs non nitrogen fixers),[9] but they also exhibit successional patterns based on season and temperature (summer blooms vs fall blooms).[10] For instance, *Microcystis* species have been documented to dominate during summer blooms, while other taxa such as *Aphanizomenon* are present during cooler weather.[11] The specter of a changing climate bodes for increases in cyanoHABs in freshwater bodies,[12] with worsening summer blooms and a potential for toxic blooms later in the fall. Increasing temperatures and nutrient regimes will impact these existing community dynamics and may alter the composition of the cyanotoxin pool during bloom events.[13]

The goal of the current work was to determine cyanobacterial community composition and toxin production alterations over time during cyanoHAB events at three urban lakes using DNA metabarcoding and untargeted metabolomics approaches. The data showed that communities shifted over time with decreasing species diversity throughout the event culminating in domination by *Aphanizomenon*. Additionally, cyanotoxins did not show constitutive production but appeared in a punctuated fashion correlating strongly with cyanobacterial biomass. As the bloom progressed, metabolite profiles shifted suggesting the production of a unique metabolite pool as species succession occurred. This work identified putative new cyanotoxins and we isolated three new microcystins (**1**−**3**) following chromatographic separation of a commercially available chromatography library. In this work, we identified microcystins containing doubly homologated amino acids as ECTs and set baseline time series data on community composition that can be augmented by future field studies. Furthermore, the data presented drive new hypotheses with respect to the effects of climate change on community composition and toxin production.

2. METHODS AND MATERIALS

2.1. Sample Sites and Sample Collection. Surface water samples were acquired weekly over the course of a cyanoHAB late bloom event at Roger Williams Park in Providence, Rhode Island (Figure S1). The cyanoHAB event was observed in three lakes at the park (Polo Lake, Pleasure Lake, and Cunliff Lake) from September 1, 2022 to December 7, 2022. One surface water sample was taken from Blackstone Pond in Cranston, RI on 9/8/2022, but weekly sampling did not continue at this site. The water samples were transported to the laboratory and chlorophyll *a* values were measured using UV absorbance following filtration of 50 mL of surface water over a GF/F filter and extraction with methanol.[14] Additional samples (30 mL) were filtered over a 47 mm 0.2 μm Sterlitech polyester track-etch (PETE) filter and stored at −80 °C for subsequent DNA extraction. A third portion of surface water (50 mL) was filtered over a 47 mm 3 μm PETE filter to capture cyanobacterial cells for toxin analysis. These filters were stored at −20 °C prior to analysis. In all, a total of 43, 46, and 44 samples were analyzed for chlorophyll *a*, cyanobacterial community, and toxin composition, respectively. Surface water data, water quality data, and additional cyanobacteria data were publicly available through https://www.stormwaterinnovation.org/data. These data included chlorophyll *a* measurements, nutrient measurements, and other abiotic parameter measurements for the time period of this study and preceding periods.

2.2. DNA Isolation and Metabarcoding. DNA was extracted from biomass collected on the 47 mm 0.2 μm Sterlitech PETE filters using a modified version of the Qiagen Plant MiniKit with 4 μL RNase-A added, a 1 min bead-beating step, and a total elution volume of 30 μL Buffer AE. For each sample, DNA was quantified using a Nanodrop 2000 prior to amplification. Gene amplifications were completed using cyanobacteria-specific primers[15] with MiSeq adapters to target a region of the 16S rRNA gene between target sites at 359 and 701 bps (Primers—CYA359 forward primer: 5′ GAA TTT TCC GCA ATG GG 3′; CYA781Ra reverse primer: 5′ GAC TAC TGG GGT ATC TAA TCC CAT T 3′; CYA781Rb reverse primer: 5′ GAC TAC AGG GGT ATC TAA TCC CTT T 3′). Amplicons were then sequenced using Illumina MiSeq Next-Generation Sequencing platform using V3 chemistry and 2 × 250 bp paired-end sequencing at the University of Rhode Island Molecular Informatics Core. Sequences were returned as demultiplexed reads. Raw reads were quality controlled before and after trimming with FastQC (v0.11.7)[16] and MultiQC (v1.14).[17] MiSeq adapters and primers were trimmed using CutAdapt (v4.4).[18] DADA2 (v1.26.0)[19] was used in the coding platform R to estimate sequencing error and to determine amplicon sequence variants (ASVs). Taxonomy was assigned using the SILVA reference database (v138.1)[20] and NCBI BLAST and ASVs determined to be chloroplast DNA, mitochondrial DNA, and unassigned sequences were removed. The processed data set of 107 ASVs across 46 samples was then imported into Phyloseq (v. 1.44.0),[21] an R package for visualization and analysis of molecular sequence data. Phyloseq was used to perform zero-replacement[22] and center-log ratio transformations on raw read abundances in accordance with current best practices for analyzing compositional data (e.g., bacterial sequences).[23] Aitchison distances were then calculated prior to Nonmetric MultiDimensional Scaling (NMDS) ordination and Analysis of Similarities (ANOSIM). Patterns in cyanobacterial species beta diversity across sample sites were examined with NMDS ordination techniques and quantitatively tested for group dispersion (permutest, R) and analysis of variance among groups (ANOSIM, PERMANOVA, R). Alpha diversity trends over time were calculated with chao1 and shannon index[24] and trends in alpha diversity over time were quantitatively assessed with the Mann−Kendall test, a statistical test for time series trends.[25] To qualitatively examine successional patterns of cyanobacterial species over time, raw read abundances were also transformed to relative abundances and plotted in phyloseq. All samples were used for the NMDS plots for every location (Cunliff, Polo, and Pleasure) to examine community composition by site. The raw sequence reads have been deposited to the Sequence Read Archive at Genbank (BioProject #: PRJNA1065459).

2.3. Toxin Analysis. The 47 mm 3 μm filters were thawed at room temperature and repeatedly extracted in 70%/25%/5% CH_3OH, H_2O, n-butanol until no color was observed in the

https://doi.org/10.1021/acsestwater.4c00266
ACS EST Water 2024, 4, 3423−3432

extract. Extracts for each sample were pooled and then concentrated in vacuo, reconstituted in CH_3OH and subjected to a sample preparation step whereby each extract was passed over a 100 mg C18 SPE cartridge eluting with 1 mL of CH_3OH directly into an LC−MS vial. Each sample was analyzed via LC−MS/MS to determine cyanotoxin composition. Raw mass spectrometry data were collected using a Dionex Ultimate 3000 high-performance liquid chromatography (HPLC) system coupled to a Thermo Scientific LTQ XL mass spectrometer. A 2.6 μm Kinetex C18 column (150 × 4.6 mm) was used for separations with a flow rate set at 0.4 mL/min. A gradient method consisting of H_2O with 0.1% formic acid and CH_3CN with 0.1% formic acid was used. The gradient method was as follows: 15% CH_3CN was held for 5 min, followed by a 15 min gradient to 100% CH_3CN, which was held for 10 min followed by a return to initial conditions from 31 to 38 min. For the data dependent MS/MS component, the CID isolation width was 1.0 and the collision energy was 35.0 eV.

2.4. LC−MS/MS-Based Molecular Networking. Once acquisitions were complete, .raw data files were exported and transformed into .mzXML format using MSConvert.[26] Files were uploaded into the Global Natural Products Social Molecular Networking platform (GNPS).[27] Network parameters included a parent mass tolerance and MS/MS fragment mass tolerance of 2.0 and 0.5 Da, respectively for low resolution data. The network's cosine score for edge connection was set to 0.6 with at least 3 matched peaks required. The spectra were searched against the GNPS library of spectra, where matched nodes needed to have at least 6 matched peaks and meet the minimum cosine score of 0.7. Library hits were annotated for each sample and verified by MS/MS fragmentation comparisons. Cyanotoxins were annotated using the GNPS platform either by specific library hits or by matches to MS/MS spectra from literature sources. Precursor m/z values of identified cyanotoxins were extracted using the GNPS Dashboard function and abundance values were annotated for each toxin.[28] To garner total metabolite counts for each sample, each file was uploaded to MSDIAL,[29] and peak lists were generated for each MS acquisition to give a list of metabolites. Correlations were performed by computing Pearson correlation coefficients in Prism (v. 9.5.1). All raw mass spectrometry files and .mzXML files are available in the MassIVE repository (accession#: MSV000093676).

2.5. Principal Component Analysis. The peak lists for all samples were aligned, and peak list tables including retention time, mass to charge ratio, and peak intensity were exported as .csv files. The peak lists were uploaded to MetaboAnalyst (v. 2.0),[30] and the default parameters for PCA analysis were used. Data were then filtered by mean intensity value and the data were Pareto scaled (mean-centered and divided by the square root of the standard deviation of each variable). Finally, PCA plots were generated to examine similarities in metabolite composition at all sites and with respect to two time periods (early: 9/1/2022 to 10/19/2022; late: 10/26/2022 to 12/7/2022).

2.6. New Toxin Isolation. To isolate new cyanotoxins in the amounts necessary for full NMR structure characterization, we purchased a chromatography library from Biosortia Microbiomics. The material in this library was derived from a cyanobacterial bloom in Muskegon, MI.[8] This library was used by our laboratory previously to isolate new antineuroinflammatory micropeptins.[31] In addition, to these antineuroinflammatories there were also chromatography fractions that showed strong cytotoxicity to murine BV-2 microglial cells.[31] We purchased preparative amounts of these fractions (ca. 3−15 mg/fraction) with the intent of isolating new cyanotoxins. We focused on fractions which showed the strongest cytotoxicity in previous bioassays (fractions D40-D67).[31] HPLC-DAD (Agilent 1260 System equipped with a vacuum degasser, autosampler, and diode array detector) and matrix-assisted laser desorption ionization time-of-flight (MALDI-TOF) (Bruker autoflex maX) indicated that these fractions contained microcystins and we focused on samples D55, D59, and D67 due to the fact that they showed strong cytotoxicity and the m/z of analytes in MALDI-TOF analysis could not be found in our literature and database searching. Analysis of fraction D55 (3 mg) by ^{1}H NMR showed it contained a single compound (**1**) and no further chromatography was needed for purification. Sample D59 was separated using a YMC 5 μm ODS column (250 × 10 mm^2) and a gradient method with H_2O and CH_3CN as mobile phase solvents each modified with 0.1% formic acid and a flow rate of 3.00 mL/min. Compounds were eluted with a gradient of CH_3CN in H_2O from 32 to 42% over 30 min followed by an increase to 100% CH_3CN to 35 min and a 100% hold of CH_3CN to 40 min with a return to initial conditions at 41 min. We isolated 2 mg of compound **2** (t_R 37.9 min). Fraction 67 was subjected to the same chromatographic separation as D59, except the gradient began at 50% CH_3CN in H_2O changing to 100% CH_3CN over 30 min followed by a 100% CH_3CN hold to 35 min and a return to initial conditions at 36 min and compound **3** was isolated (2 mg, t_R 16.5 min). Characterization was accomplished using MALDI-TOF and NMR (500 MHz, Bruker Ascend AVANCE III HD) and chemical shifts reported for compounds **1**−**3** were referenced to the residual solvent peaks of DMSO-d_6 (δ_H 2.50 and δ_C 39.5) or methanol-d_4 (δ_H 3.31and 4.78 and δ_C 49.2). For physical data on compounds **1**−**3**, see the Supporting Information. Raw NMR data for **1**−**3** has been deposited at NP-MRD (https://np-mrd.org/; **1**: NP0333533; **2**: NP0333531; **3**: NP0333532).

3. RESULTS AND DISCUSSION

3.1. Fall CyanoHABs in Urban Lakes. CyanoHABs were observed at the three study sites on the first day of sampling (September 1, 2022), and cyanobacterial cell density increased over time in these water bodies as observed by photography, analysis of water samples by microscopy, and by examination of chlorophyll *a* values (Figures S2−S5). Biomass maxima were reached on November 2, 2022, at Pleasure and Cunliff Lakes, while the biomass maximum was reached on October 19, 2022, at Polo Lake (Figure S5). We ended sampling on December 14, 2022, after seeing no cyanobacterial cells in surface water samples from two sites (Pleasure and Cunliff Lakes). However, we should note that with respect to the entire bloom timeline at these sites, our samples represent the later bloom period as chlorophyll *a* measurements from these lakes showed a spring/summer bloom beginning in May 2022, reaching a maximum in July and decreasing through the rest of the summer before our sampling period began in early September (Figure S6). Surface samples were processed in the laboratory for chlorophyll *a* analysis, DNA metabarcoding, and toxin analysis. *Microcystis aeruginosa* NIES-933 (UTEX LB 2385) was purchased from the UTEX culture collection (a known MC-LR producer) and served as a positive control for both molecular sequencing and toxin analysis. Following

https://doi.org/10.1021/acsestwater.4c00266
ACS EST Water 2024, 4, 3423−3432

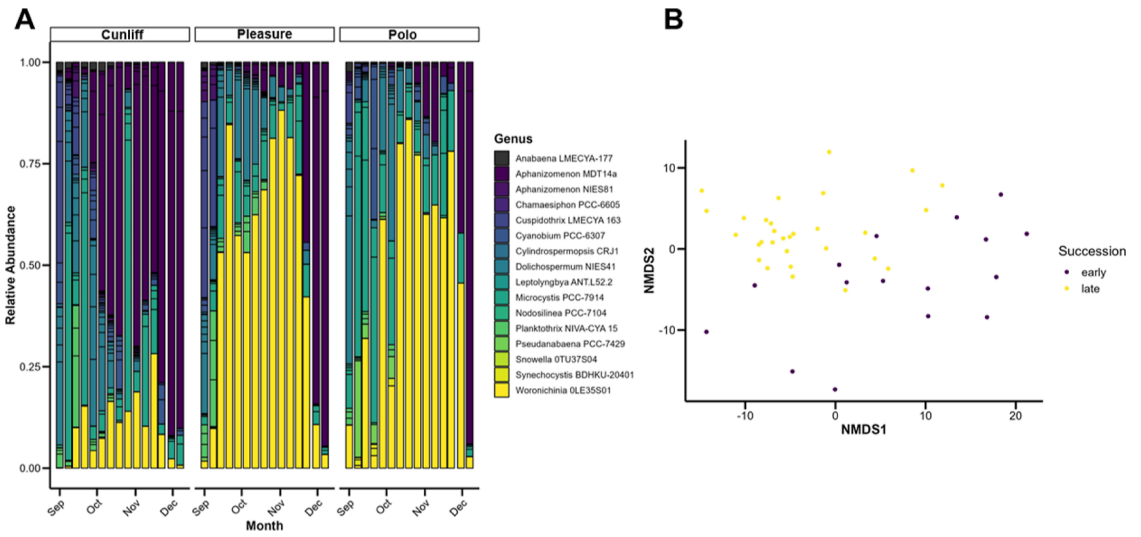

Figure 1. (A) CyanoHAB community composition and successional patterns. Relative abundances of cyanobacterial taxa at Cunliff, Pleasure, and Polo Lakes from 9/1/2022 to 12/7/2022. (B) NMDS plots of the cyanobacterial taxa composition at all sites for early and late bloom periods. There was significant difference observed in the similarity of community composition in the two periods (ANOSIM, $p < 0.001$, $R = 0.586$).

microscopy analysis of environmental samples, community shifts were noted from early to late bloom periods with the identification of *Aphanizomenon* colonies in late November and December samples (Figure S4). These observations were further supported by subsequent molecular analysis (see below).

3.2. Cyanobacterial Species Distribution across Space and Time. Examination of cyanobacterial relative abundances at the genus level showed a distinct successional pattern over the study period at all three sites. Diverse filamentous species such as *Cuspidothrix* sp., *Dolichospermum* sp., and *Planktothrix* sp. were observed during the first 2 weeks of sampling with *Microcystis* and *Woronichinia* sp. (family Microcystaceae) codominating the remainder of the earlier and middle bloom periods (9/14/2022−11/2022). *Aphanizomenon* sp. (family Nostocaceae) showed the highest relative abundance during the later bloom, with complete community dominance by 11/30/2022 (Figure 1A). Cunliff Lake showed lower relative levels of *Woronichinia* compared to the other two lakes and the presence and relative abundance of *Aphanizomenon* sp. occurred earlier (Figure 1A). NMDS ordination showed enough separation between the composition of the cyanobacterial community between September and October to December (stress = 0.132, dimensions = 2) to delineate two succession "stages" in the late bloom, which we classified as "early" and "late" (Figure 1B). This separation was supported by tests of variance between the grouping of succession and genus (ANOSIM, $p < 0.001$, $R = 0.586$). However, permutation tests showed significant dispersion within the succession grouping ($p < 0.05$), and the succession groups identified still contained some overlap and a high degree of scatter. Sample sites differed in taxonomic composition (ANOSIM, $R = 0.14$, $p < 0.01$), with this difference driven by Cunliff Lake, though again permutation tests revealed a significant amount of dispersion ($p < 0.01$) (Figure S7). Examining cyanobacterial genera by site, Cunliff Lake was the most unique and was dominated more by *Microcystis* than *Woronichinia* in the early bloom period and then dominated by *Aphanizomenon* earlier in the time series compared to Polo and Pleasure Lakes (Figure 1A). The positive control (UTEX LB 2385, *M. aeruginosa* NIES-933) ASVs were identified as 100% *Microcystis* following our bioinformatics analysis, and the sequence match was 100% to *M. aeruginosa* NIES 933 (Figure S8A). Additionally, MC-LR was detected in extracts of this strain with an MS/MS match to that of the MC-LR in the GNPS library (Figure S8B).

The cyanobacterial community was more diverse at the onset of the bloom and diversity decreased as the bloom progressed by both chao1 (richness) and shannon (richness and evenness) metrics across all sample sites (Figure 2).

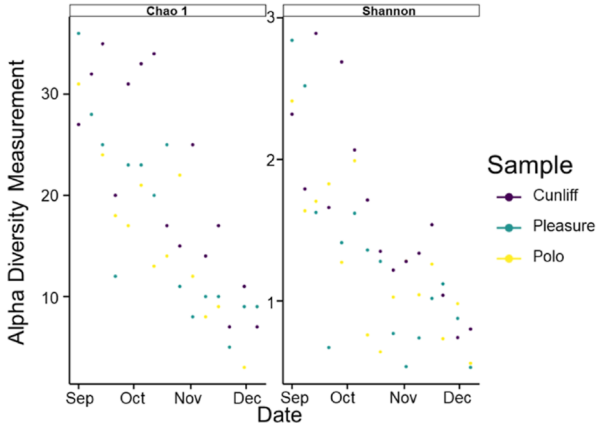

Figure 2. Species diversity decreased over the course of cyanoHABs. Alpha diversity measurement of individual discrete samples from field sites completed over the time period 9/1/2022 to 12/7/2022 determined by Chao and Shannon metrics.

Mann−Kendall test results showed that these decreases over time were significant across all metrics (chao/tau = −0.61, $p < 0.001$; shannon/tau = −0.19, $p < 0.001$). The use of DNA barcoding for community analysis instead of cell counts likely increased the species resolution over the course of the bloom and allowed for a clear picture of decreasing species diversity as the cyanoHABs progressed.

The molecular community composition data are consistent with past work done using cell counts and cultivation studies.

https://doi.org/10.1021/acsestwater.4c00266
ACS EST Water 2024, 4, 3423−3432

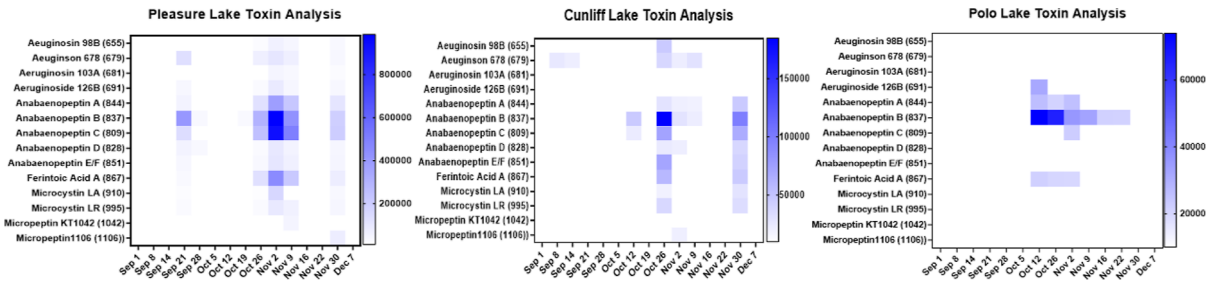

Figure 3. Cyanotoxin annotation and relative concentration at Pleasure, Cunliff, and Polo Lakes during the study period from 9/1/2022 to 12/7/2022. The colors in the heat maps are proportional to the intensity of the extracted ion for each analyte. Precursor masses for each toxin are listed in the parentheses.

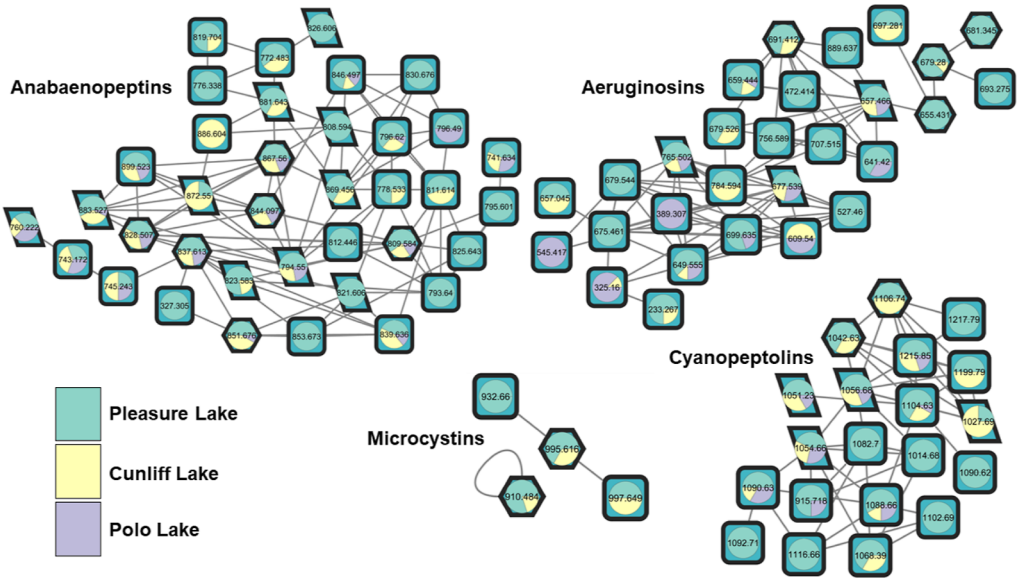

Figure 4. LC−MS/MS network of all extracts from surface water samples during the study period. Nodes are designated by their precursor m/z values (e.g., 995.616 is the precursor m/z value for microcystin-LR) and grouped into toxin classes. Pie slices indicate in which lake metabolites were detected (Pleasure, green; Cunliff, yellow; Polo, purple). Hexagons indicate that metabolites were among the 14 annotated in the study, while parallelograms indicate metabolites that are putatively known but were not specifically monitored. Squares indicate putatively new toxins.

Multiple studies have shown changing cyanobacterial successional patterns either from *Aphanizomenon* sp. to *Microcystis* or vice versa likely driven by temperature and this pattern can oscillate seasonally.[9,10,32,33] Culture studies have shown that *Microcystis* sp. has a higher maximum growth rate at warmer temperatures than *Aphanizomenon* sp.[34] In this study, strong correlations were found between decreasing temperature and increasing *Aphanizomenon* relative abundance at the study sites (Figure S9A,B). Additionally, significant correlations were observed between decreasing temperature and decreasing biomass and decreasing species diversity (Figure S9C,D). We did not find significant relationships between TN and TP and *Aphanizomenon* abundance, biomass levels, and diversity. These observations were consistent with previously work that showed that temperature was one of the strongest explanatory variables for cyanobacterial biomass in lakes and they were consistent with *Aphanizomenon*'s behavior in culture with respect to temperature.[34,35] However, *Aphanizomenon*'searly abundance at Cunliff Lake can likely not be explained simply by temperature as the temperature was no different at Cunliff than the other lakes. In addition to temperature, nitrogen source and N/P ratio play significant roles in shaping cyanobacterial community succession (review in Tanvir et al. 2021).[10] In this study, nutrient data were obtained for Polo Lake during the study period, but not Cunliff and Pleasure although there were historical nutrient data for these sites available at https://www.stormwaterinnovation.org/data. Nitrogen and phosphorus levels at Polo Lakes generally mirrored cyanobacterial biomass levels from the spring until winter (Figure S9E). Cyanobacterial biomass and toxin abundance can be controlled by both N and P and additionally the speciation of N as ammonia or nitrate concentrations can favor certain taxa and nondiazotrophs versus diazotrophs.[36,37] While we were limited in the amount of nutrient data collected, we did find that biomass maxima and a maximum in toxin production occurred at dates with the highest N/P ratios (cf. Figures 3, S5, and S9F) and ammonia and the ammonia/nitrate ratio decreased throughout the study period. However, there were only two dates measured throughout the study period, which limited any measurement of significance. These nutrient factors play a role in community composition and toxin production and there are many other abiotic parameters to considered which were not measured in this study such as iron and sulfate.[38] Furthermore, it is important to note that we only examined the cyanobacterial community in blooms and the heterotrophic bacterial community plays a role in these events by enhancing cyanobacterial growth, metabolizing cyanobacterial compounds, and cycling nutrients.[39]

https://doi.org/10.1021/acsestwater.4c00266
ACS EST Water 2024, 4, 3423−3432

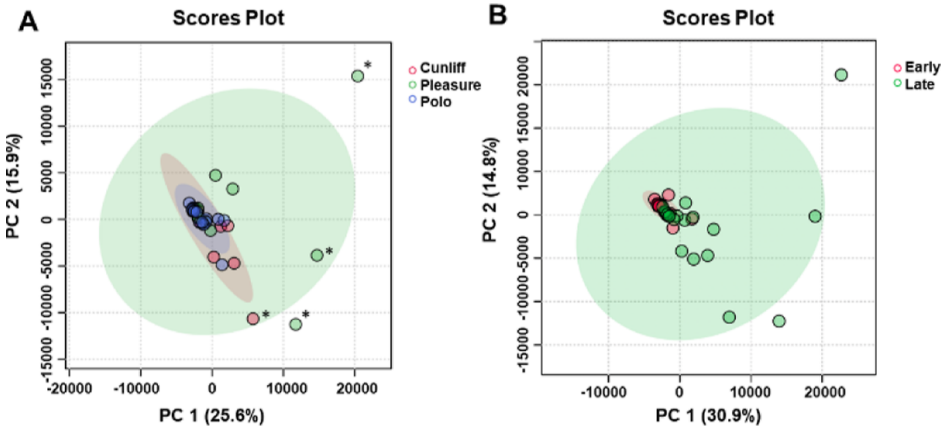

Figure 5. PCA analysis of bloom metabolites. (A) Comparison by site showed similarities in metabolite profiles among all sites. Asterisks show outliers (top to bottom: Pleasure 11/2/2022; Pleasure 11/9/2022; Cunliff 11/9/2022; Pleasure 11/30/2022. (B) Separating by early and late bloom periods showed differences in metabolite profiles.

Previous studies have shown spatial−temporal variation in community composition and toxin production,[33,40] while we showed very clear temporal variation and some spatial variation. This lack of spatial variation may be due to the proximity of the sites used in the study and some connection of water masses among the lakes. The study site lakes were likely subjected to similar nutrient regimes and other abiotic and biotic parameters. Our results suggest that more research should be devoted to the genus *Woronichinia*. This group showed abundance throughout most of the bloom period at two lakes, correlated with the relative abundance of *Microcystis* sp. at Pleasure Lake (Figure S10), and its high abundance in urban lakes has been previously reported.[41] While this genus does not appear to possess MC biosynthetic genes, clusters for the anabaenopeptins and other cyanopeptides have been annotated.[42] Some toxicity from this group has been reported against invertebrates,[43] and further investigation of its ecological role and its potential for allelopathic compound production is warranted.

3.3. Cyanotoxin Production during Blooms and the Isolation of New Microcystins. We annotated 14 known cyanotoxins from LC−MS/MS data. Microcystin-LR, MC-LA, anabaenopeptin A, and ferintoic acid A were identified using the library search function at GNPS and our putative toxin queries were matched to MS/MS fragmentation patterns for library compounds (Figure S11). Microcystin-LR identified in our environmental samples had an identical retention time, precursor m/z and MS/MS fragmentation pattern to that of the MC-LR identified in the UTEX positive control (Figure S11). Additional toxins were identified by examining MS/MS networks (e.g., anabaenopeptin B in same cluster as anabaenopeptin A) and by comparing precursor m/z values and MS/MS spectra to previously published work.[44−47] Toxin concentrations (as determined by AUC values from mass spec data) coincided with cyanobacterial biomass maxima at all three lakes (Figures 3 and S12A) and toxin production was not constitutive. Additionally, metabolite content in general increased with cyanobacterial biomass (Figure S12B).

Examination of LC−MS/MS networks annotated multiple toxin classes (e.g., microcystins, anabaenopeptins, aeruginosins, and cyanopeptolins) and putative new toxins, but hundreds of metabolites remain to be annotated demonstrating that these events are incredibly chemically complex (Figure 4). The LC−MS/MS networking approach to identify new cyanopeptides and toxins has shown utility,[48] and this strategy is well suited to define structure−activity relationships among toxin classes. Most of the toxins of interest were found at all three lakes (e.g., anabaenopeptins A, B, and ferintoic acid B), but interestingly MC-LR was only detected in samples collected from Pleasure and Cunliff Lakes. Examining metabolite content over the entire sample period and all sites by PCA, we observed very similar composition overall (Figure 5A). However, delineating samples by early and late periods of the bloom, there was a difference in composition driven by the presence and concentration of cyanotoxins (Figure 5B). In terms of connecting specific cyanobacterial taxa to toxin production, there was a high relative abundance of *Microcystis* at Cunliff Lake on 10/26/22 which coincides with the highest abundances of MCs and other cyanotoxins (cf. Figures 1A and 3). However, there were high levels of *Microcystis* observed at Polo Lake early in the bloom period with no corresponding MCs detected, which may be explained by a complicated array of potential triggering factors such as nutrient profiles, competition, heterotrophic bacterial activity, and grazing, among others. The metabolomics data we reported were consistent with metatranscriptomics studies that showed *mcy* and other toxin biosynthesis genes were generally expressed during the later part of blooms.[49,50] However, this picture is complicated by the number of toxin producing taxa present in cyanoHABs and their ecosystem function and population dynamics. Integrating more 'omics approaches such as metagenomics and metatranscriptomics with the metabolomics data will give greater insight into the ecophysiological roles of cyanotoxins in shaping cyanobacterial and bacterial communities.

Initial attempts to mine through extracts and chromatography fractions from Polo, Pleasure, and Cunliff Lakes proved to be futile for full structure characterizations as we did not collect enough biomass to isolate low abundance components in extracts and fractions. Thus, we mined through a chromatography fraction library purchased from Biosortia Microbiomics with the intent to isolate new microcystins and cyanotoxins from fractions that showed potent cytotoxicity to BV-2 microglial cells in previous work.[31] Initial HPLC-DAD analysis of active fractions showed the presence of analytes with a UV maximum at 238 nm, which was consistent with microcystins (Figure S13A). Following MALDI-TOF analysis of chromatography fractions, we identified three analytes for

https://doi.org/10.1021/acsestwater.4c00266
ACS EST Water 2024, 4, 3423−3432

isolation that did not match with m/z values in our available databases (m/z 1144, m/z 1064, and m/z 1050) (Figure S13B). These putative new toxins were isolated using HPLC and characterized by NMR analysis, which consisted of examining ^{1}H NMR, HSQC, COSY, TOCSY, and ROESY spectra (Figures S14−S25). For compounds **1** and **2**, we constructed the core microcystin structure of (2*S*,3*S*,8*S*,9*S*)-3-amino-9-methoxy-2,6,8-trimethyl-10-phenyldeca-4,6-dienoic acid (ADDA), D-glutamate, *N*-methyldehydroalanine (Mdha), D-alanine, and D-methylaspartate (Masp) leaving position X and Z (the variable positions) unassigned. MALDI-TOF analysis of **1** gave an m/z value of 1144.5520 $[M + Na]^+$, which suggested a molecular formula of $C_{60}H_{79}N_7O_{14}$. This molecular formula was 14 Da higher than a previously characterized microcystin with two bis-homologated tyrosine (bHtyr) residues at the variable positions.[8] Examination of the ^{1}H NMR showed only one signal difference from MC-bHtyr−bHtyr in the presence of a deshielded singlet at δ_H 3.59 (CH_3), which strongly suggested the presence of a second methoxy group.[51] We hypothesized that this modification was in the form of a methyl ester as an O-methylation on a bis-homologated tyrosine residue would likely feature a more deshielded signal around δ_H 3.80.[52] Comparing the ^{13}C NMR data derived from the HSQC spectrum of **1** to that of the previously characterized MC-bHtyr−bHtyr[8] showed larger chemical shift differences for the D-Glu[6] residue (Δ 2.6 ppm) compared to the Masp residue (Δ 0.4 ppm), and [D-Glu(OMe)[6] has been described previously in both isolated microcystins and synthesized microcystins.[53,54] Thus, the molecule was characterized as a microcystin with two bis-homologated tyrosine residues at the variable positions and a glutamate methyl ester (Figure 6). The glutamate is much more easily methylated than the methylaspartic acid residue in methylation procedures,[54] and it may be that this molecule is an artifact of the isolation process rather than a biosynthetic microcystin.[55] However, it will still be interesting to examine how this modification affects hepatotoxicity and transport in future studies.

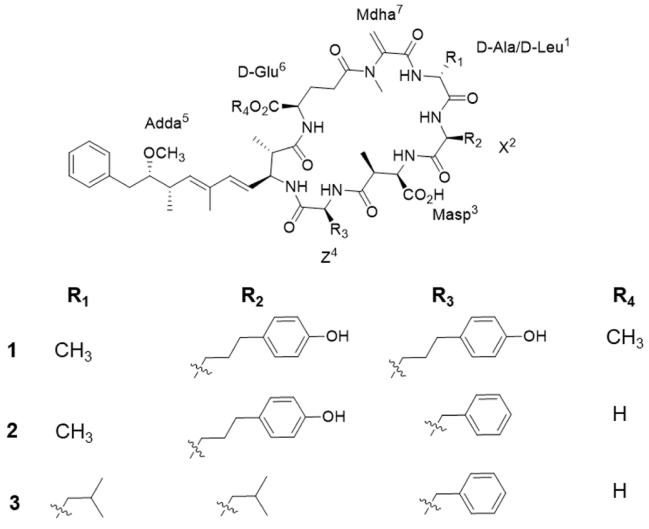

Figure 6. Structures of compounds **1**−**3**.

MALDI-TOF analysis of compound **2** gave an m/z value of 1086.5170 $[M + Na]^+$ suggesting a molecular formula of $C_{57}H_{73}N_7O_{13}$. The focus for characterization was on the amino acids at the variable positions as the core structure was established through examination of the HSQC and TOCSY spectra. A TOCSY spin system showing correlations of three methylene protons to the α proton of the amino acid side chain [δ_H 4.43 (CH) and δ_H 2.05 (CH_2), 1.54 (CH_2), and 2.47 (CH_2)], and a ROESY correlation between a methylene in this amino acid (δ_H 1.54) and the methyl group in D-alanine (δ_H 1.13) strongly suggested a bHtyr residue at position 2, and a spin system between δ_H 4.36 (CH) and δ_H 3.19 and 2.97 (CH_2) strongly supported a phenylalanine residue at position 4 and completed the structure of **2** (Figure 6).

MALDI-TOF analysis of compound **3** gave an m/z value of 1050.5547 $[M + Na]^+$ suggesting a molecular formula of $C_{55}H_{77}N_7O_{12}$. The ADDA, D-Glu, Mdha, and Masp were established from examination of the HSQC and TOCSY data. However, instead of an alanine residue at position one, there were two ^{1}H−^{1}H spin systems consistent with two leucine residues (positions 1 and 2) and a correlation between a methine proton δ_H 4.48 and a methylene (δ_H 3.35 and 2.69) strongly suggested a phenylalanine residue at position 4. ROESY correlations between δ_H 1.56 (CH_2) in leucine[2] and δ_H 0.85 (CH_3) in leucine-1 and a ROESY correlation between δ_H 1.69 in leucine[1] and δ_H 5.40 in Mdha established the sequence of these residues in the molecule. The absolute configuration of all three molecules is proposed by analogy to the conventional microcystin structure configuration.

4. CONCLUSION

Our current report provokes intriguing questions as to the ecological relationship between *Aphanizomenon* and *Microcystis* in terms of *Aphanizomenon*'s potential control of *Microcystis* growth and toxin production or if the relationship is primarily driven by temperature adaptation. While there are multiple studies pointing to allelopathic effects of *Microcystis* metabolites on *Aphanizomenon*,[11,56] there is a gap in knowledge on the effect of *Aphanizomenon*'s metabolites on *Microcystis*. Future work will consist of coculture experiments with these two organisms and the isolation, structure elucidation, and biological evaluation of putative new toxins from known classes and those from potentially novel classes with special attention to those microcystins with homologated and doubly homologated amino acid residues. The potential aquatic toxicity and human health effects from emerging toxins and nonmicrocystin toxins have been well described in fish models with nonmicrocystin containing extracts and extracts from nonmicrocystin producing cyanobacterial strains still causing significant aquatic toxicity.[57] Certain micropeptins have been shown to cause mortality and morbidity effects in fish models,[57] and more research is needed to understand the full toxin suite in cyanoHAB events and their potential organismal effects. More community and toxin composition data from various environments will provide predictive tools with the biological and chemical data needed to forecast these events to a greater extent.[58] This will necessitate including the heterotrophic bacterial community and determining the impact that these organisms have on bloom biomass and cyanotoxin production. Having isolated three new microcystins (**1**−**3**) and showing an abundance of potential new cyanopeptides in LC−MS/MS molecular networking analysis, mixture analyses will be necessary to understand the combined effects of cyanotoxins on biological end points. Microcystins with unusual homologated amino acids and [D-Leu][1] may be overlooked with respect to microcystin composition in blooms.

https://doi.org/10.1021/acsestwater.4c00266
ACS EST Water 2024, 4, 3423−3432

Additionally, our data suggest that reducing cyanobacterial biomass in general rather than controlling for specific harmful groups will likely reduce all metabolites produced including toxins.

■ ASSOCIATED CONTENT

Supporting Information

The Supporting Information is available free of charge at https://pubs.acs.org/doi/10.1021/acsestwater.4c00266.

Supporting Information with photographs and micrographs of cyanoHAB samples, chlorophyll *a* values, additional NMDS plots, data on specialized metabolites correlated with cyanobacterial biomass, and NMR data (PDF)

■ AUTHOR INFORMATION

Corresponding Author

Matthew J. Bertin − *Department of Chemistry, Case Western Reserve University, Cleveland, Ohio 44106, United States;* orcid.org/0000-0002-2200-0277; Email: mxb1224@case.edu

Authors

Julie A. Maurer − *Department of Cell and Molecular Biology, University of Rhode Island, Kingston, Rhode Island 02881, United States*

Runjie Xia − *Department of Chemistry, Case Western Reserve University, Cleveland, Ohio 44106, United States*

Andrew M. Kim − *Department of Biomedical and Pharmaceutical Sciences, College of Pharmacy, University of Rhode Island, Kingston, Rhode Island 02881, United States*

Nana Oblie − *Department of Biomedical and Pharmaceutical Sciences, College of Pharmacy, University of Rhode Island, Kingston, Rhode Island 02881, United States*

Sierra Hefferan − *Department of Biomedical and Pharmaceutical Sciences, College of Pharmacy, University of Rhode Island, Kingston, Rhode Island 02881, United States*

Hannuo Xie − *Department of Chemistry, Case Western Reserve University, Cleveland, Ohio 44106, United States*

Angela Slitt − *Department of Biomedical and Pharmaceutical Sciences, College of Pharmacy, University of Rhode Island, Kingston, Rhode Island 02881, United States*

Bethany D. Jenkins − *Department of Cell and Molecular Biology, University of Rhode Island, Kingston, Rhode Island 02881, United States; Graduate School of Oceanography, University of Rhode Island, Narragansett, Rhode Island 02882, United States*

Complete contact information is available at: https://pubs.acs.org/10.1021/acsestwater.4c00266

Author Contributions

[⊥]J.A.M. and R.X. contributed equally. M.B. and A.S. conceived the study. J.M., R.X., A.M.K., N.O., S.H., and H.X. performed data acquisition and conducted data analysis. B.J. provided materials and analysis and interpretation of data. M.B. wrote the manuscript with contributions of all authors. All authors have given approval to the final version of the manuscript. CRediT: **Julie Maurer** data curation, formal analysis; **Runjie Xia** formal analysis, writing-review & editing; **Andrew M Kim** data curation, formal analysis, methodology; **Nana Oblie** data curation, formal analysis; **Sierra Hefferan** data curation, formal analysis; **Hannuo Xie** formal analysis, software, visualization.

Funding

Research reported in this article was supported by the National Institute of Environmental Health Sciences of the National Institutes of Health under award number R21ES033758 (M.J.B. and A.S.). The content is solely the responsibility of the authors and does not necessarily represent the official views of the National Institutes of Health. The research was also supported in part by the National Science Foundation under award number 2320090.

Notes

The authors declare no competing financial interest.

■ ACKNOWLEDGMENTS

We are grateful to the members of the Stormwater Innovation Center, especially Ryan Kopp, Arthur Gold, and Elizabeth Herron, for helpful conversations and about the lakes at Roger Williams Park and direction on publicly available data. Acquisition of certain data in this publication was made possible by the use of equipment and services available through the RI-INBRE Centralized Research Core Facility at the University of Rhode Island, which is supported by the Institutional Development Award (IDeA) Network for Biomedical Research Excellence from the National Institute of General Medical Sciences of the National Institutes of Health under grant number P20GM103430.

■ REFERENCES

(1) He, J.; Li, G.; Chen, J.; Lin, J.; Zeng, C.; Chen, J.; Deng, J.; Xie, P. Prolonged Exposure to Low-dose Microcystin Induces Nonalcoholic Steatohepatitis in Mice: A Systems Toxicology Study. *Arch. Toxicol.* **2017**, *91* (1), 465−480.

(2) Falconer, I. R.; Beresford, A. M.; Runnegar, M. T. Evidence of Liver Damage by Toxin from a Bloom of the Blue-green Alga, Microcystis aeruginosa. *Med. J. Aust.* **1983**, *1* (11), 511−514.

(3) Redfern, R.; Micham, J.; Daniels, R.; Childers, S. Something in the Water: Hospital Responds to Water Crisis. *Disaster Med. Public Health Prep.* **2018**, *12* (5), 666−668.

(4) Chorus, I.; Welker, M. *Toxic Cyanobacteria in Water—A Guide to Their Public Health Consequences, Monitoring and Management*, 2nd ed.; CRC Press, Boca Raton, FL on behalf of the World Health Organization (WHO): Geneva, CH, 2021.

(5) Jones, M. R.; Pinto, E.; Torres, M. A.; Dörr, F.; Mazur-Marzec, H.; Szubert, K.; Tartaglione, L.; Dell'Aversano, C.; Miles, C. O.; Beach, D. G.; McCarron, P.; Sivonen, K.; Fewer, D. P.; Jokela, J.; Janssen, E. M. L. CyanoMetDB, a Comprehensive Public Database of Secondary Metabolites from Cyanobacteria. *Water Res.* **2021**, *196* (15), 117017.

(6) Nugumanova, G.; Ponomarev, E. D.; Askarova, S.; Fasler-Kan, E.; Barteneva, N. S. Freshwater Cyanobacterial Toxins, Cyanopeptides and Neurodegenerative Diseases. *Toxins* **2023**, *15* (3), 233.

(7) He, H.; Bertin, M. J.; Wu, S.; Wahome, P.; Beauchesne, K. R.; Youngs, R.; Zimba, P. V.; Moeller, P. D. R.; Sauri, J.; Carter, G. T. Cyanobufalins: Cardioactive Toxins from Cyanobacterial Blooms. *J. Nat. Prod.* **2018**, *81*, 2576−2581.

(8) He, H.; Wahome, P. G.; Bertin, M. J.; Pedone, A. C.; Beauchesne, K. R.; Moeller, P. D. R.; Carter, G. T.; Carter, G. T. Microcystins Containing Doubly Homologated Tyrosine Residues from a *Microcystis aeruginosa* Bloom: Structures and Cytotoxicity. *J. Nat. Prod.* **2018**, *81*, 1368−1375.

(9) Paerl, H. W.; Otten, T. G. Duelling 'CyanoHABs': Unraveling the Environmental Drivers Controlling Dominance and Succession among Diazotrophic and Non N_2-Fixing Harmful Cyanobacteria. *Environ. Microbiol.* **2016**, *18* (2), 316−324.

(10) Tanvir, R. U.; Hu, Z.; Zhang, Y.; Lu, J. Cyanobacterial Community Succession and Associated Cyanotoxin Production in

Hypereutrophic and Eutrophic Freshwaters. *Environ. Pollut.* **2021**, *290*, 118056.
(11) Ma, H.; Wu, Y.; Gan, N.; Zheng, L.; Li, T.; Song, L. Growth Inhibitory Effect of *Microcystis* on *Aphanizomenon flos-aquae* Isolated from Cyanobacteria Bloom in Lake Dianchi, China. *Harmful Algae* **2015**, *42*, 43−51.
(12) Chapra, S. C.; Boehlert, B.; Fant, C.; Bierman, V. J.; Henderson, J.; Mills, D.; Mas, D. M. L.; Rennels, L.; Jantarasami, L.; Martinich, J.; Strzepek, K. M.; Paerl, H. W. Climate Change Impacts on Harmful Algal Blooms in U.S. Freshwaters: A Screening-Level Assessment. *Environ. Sci. Technol.* **2017**, *51* (16), 8933−8943.
(13) Merder, J.; Harris, T.; Zhao, G.; Stasinopoulos, D. M.; Rigby, R. A.; Michalak, A. M. Geographic Redistribution of Microcystin Hotspots in Response to Climate Warming. *Nat. Water* **2023**, *1* (10), 844−854.
(14) Warren, C. R. Rapid Measurement of Chlorophylls with a Microplate Reader. *J. Plant Nutr.* **2008**, *31* (7), 1321−1332.
(15) Nübel, U.; Garcia-Pichel, F.; Muyzer, G. PCR Primers to Amplify 16S rRNA Genes from Cyanobacteria. *Appl. Environ. Microbiol.* **1997**, *63* (8), 3327−3332.
(16) Andrews, S. *FastQC: A Quality Control Tool for High Throughput Sequence Data*, 2010. Available online at: http://www.bioinformatics.babraham.ac.uk/projects/fastqc.
(17) Ewels, P.; Magnusson, M.; Lundin, S.; Käller, M. MultiQC: Summarize Analysis Results for Multiple Tools and Samples in a Single Report. *Bioinformatics* **2016**, *32* (19), 3047−3048.
(18) Martin, M. Cutadapt Removes Adapter Sequences from High-Throughput Sequencing Reads. *EMBnet. J.* **2011**, *17* (1), 10.
(19) Callahan, B. J.; McMurdie, P. J.; Rosen, M. J.; Han, A. W.; Johnson, A. J. A.; Holmes, S. P. DADA2: High-Resolution Sample Inference from Illumina Amplicon Data. *Nat. Methods* **2016**, *13* (7), 581−583.
(20) Quast, C.; Pruesse, E.; Yilmaz, P.; Gerken, J.; Schweer, T.; Yarza, P.; Peplies, J.; Glöckner, F. O. The SILVA Ribosomal RNA Gene Database Project: Improved Data Processing and Web-Based Tools. *Nucleic Acids Res.* **2012**, *41* (D1), D590−D596.
(21) McMurdie, P. J.; Holmes, S. Phyloseq: An R Package for Reproducible Interactive Analysis and Graphics of Microbiome Census Data. *PLoS One* **2013**, *8* (4), No. e61217.
(22) Lubbe, S.; Filzmoser, P.; Templ, M. Comparison of Zero Replacement Strategies for Compositional Data with Large Numbers of Zeros. *Chemom. Intell. Lab. Syst.* **2021**, *210*, 104248.
(23) Gloor, G. B.; Macklaim, J. M.; Pawlowsky-Glahn, V.; Egozcue, J. J. Microbiome Datasets Are Compositional: And This Is Not Optional. *Front. Microbiol.* **2017**, *8*, 2224.
(24) Kers, J. G.; Saccenti, E. The Power of Microbiome Studies: Some Considerations on Which Alpha and Beta Metrics to Use and How to Report Results. *Front. Microbiol.* **2022**, *12*, 796025.
(25) Kendall, M. G. *Rank Correlation Methods*, 4th ed.; Charles Griffin: London, 1975.
(26) Chambers, M. C.; Maclean, B.; Burke, R.; Amodei, D.; Ruderman, D. L.; Neumann, S.; Gatto, L.; Fischer, B.; Pratt, B.; Egertson, J.; Hoff, K.; Kessner, D.; Tasman, N.; Shulman, N.; Frewen, B.; Baker, T. A.; Brusniak, M.-Y.; Paulse, C.; Creasy, D.; Flashner, L.; Kani, K.; Moulding, C.; Seymour, S. L.; Nuwaysir, L. M.; Lefebvre, B.; Kuhlmann, F.; Roark, J.; Rainer, P.; Detlev, S.; Hemenway, T.; Huhmer, A.; Langridge, J.; Connolly, B.; Chadick, T.; Holly, K.; Eckels, J.; Deutsch, E. W.; Moritz, R. L.; Katz, J. E.; Agus, D. B.; MacCoss, M.; Tabb, D. L.; Mallick, P. A Cross-Platform Toolkit for Mass Spectrometry and Proteomics. *Nat. Biotechnol.* **2012**, *30* (10), 918−920.
(27) Wang, M.; Carver, J. J.; Phelan, V. V.; Sanchez, L. M.; Garg, N.; Peng, Y.; Nguyen, D. D.; Watrous, J.; Kapono, C. A.; Luzzatto-Knaan, T.; Porto, C.; Bouslimani, A.; Melnik, A. V.; Meehan, M. J.; Liu, W.-T.; Crüsemann, M.; Boudreau, P. D.; Esquenazi, E.; Sandoval-Calderón, M.; Kersten, R. D.; Pace, L. A.; Quinn, R. A.; Duncan, K. R.; Hsu, C.-C.; Floros, D. J.; Gavilan, R. G.; Kleigrewe, K.; Northen, T.; Dutton, R. J.; Parrot, D.; Carlson, E. E.; Aigle, B.; Michelsen, C. F.; Jelsbak, L.; Sohlenkamp, C.; Pevzner, P.; Edlund, A.; McLean, J.; Piel, J.; Murphy, B. T.; Gerwick, L.; Liaw, C.-C.; Yang, Y.-L.; Humpf, H.-U.; Maansson, M.; Keyzers, R. A.; Sims, A. C.; Johnson, A. R.; Sidebottom, A. M.; Sedio, B. E.; Klitgaard, A.; Larson, C. B.; Boya, P. C. A.; Torres-Mendoza, D.; Gonzalez, D. J.; Silva, D. B.; Marques, L. M.; Demarque, D. P.; Pociute, E.; O'Neill, E. C.; Briand, E.; Helfrich, E. J. N.; Granatosky, E. A.; Glukhov, E.; Ryffel, F.; Houson, H.; Mohimani, H.; Kharbush, J. J.; Zeng, Y.; Vorholt, J. A.; Kurita, K. L.; Charusanti, P.; McPhail, K. L.; Nielsen, K. F.; Vuong, L.; Elfeki, M.; Traxler, M. F.; Engene, N.; Koyama, N.; Vining, O. B.; Baric, R.; Silva, R. R.; Mascuch, S. J.; Tomasi, S.; Jenkins, S.; Macherla, V.; Hoffman, T.; Agarwal, V.; Williams, P. G.; Dai, J.; Neupane, R.; Gurr, J.; Rodríguez, A. M. C.; Lamsa, A.; Zhang, C.; Dorrestein, K.; Duggan, B. M.; Almaliti, J.; Allard, P.-M.; Phapale, P.; Nothias, L.-F.; Alexandrov, T.; Litaudon, M.; Wolfender, J.-L.; Kyle, J. E.; Metz, T. O.; Peryea, T.; Nguyen, D.-T.; VanLeer, D.; Shinn, P.; Jadhav, A.; Müller, R.; Waters, K. M.; Shi, W.; Liu, X.; Zhang, L.; Knight, R.; Jensen, P. R.; Palsson, B. Ø.; Pogliano, K.; Linington, R. G.; Gutiérrez, M.; Lopes, N. P.; Gerwick, W. H.; Moore, B. S.; Dorrestein, P. C.; Bandeira, N. Sharing and Community Curation of Mass Spectrometry Data with Global Natural Products Social Molecular Networking. *Nat. Biotechnol.* **2016**, *34* (8), 828−837.
(28) Petras, D.; Phelan, V. V.; Acharya, D.; Allen, A. E.; Aron, A. T.; Bandeira, N.; Bowen, B. P.; Belle-Oudry, D.; Boecker, S.; Cummings, D. A.; Deutsch, J. M.; Fahy, E.; Garg, N.; Gregor, R.; Handelsman, J.; Navarro-Hoyos, M.; Jarmusch, A. K.; Jarmusch, S. A.; Louie, K.; Maloney, K. N.; Marty, M. T.; Meijler, M. M.; Mizrahi, I.; Neve, R. L.; Northen, T. R.; Molina-Santiago, C.; Panitchpakdi, M.; Pullman, B.; Puri, A. W.; Schmid, R.; Subramaniam, S.; Thukral, M.; Vasquez-Castro, F.; Dorrestein, P. C.; Wang, M. GNPS Dashboard: Collaborative Exploration of Mass Spectrometry Data in the Web Browser. *Nat. Methods* **2022**, *19* (2), 134−136.
(29) Tsugawa, H.; Cajka, T.; Kind, T.; Ma, Y.; Higgins, B.; Ikeda, K.; Kanazawa, M.; VanderGheynst, J.; Fiehn, O.; Arita, M. MS-DIAL: Data-Independent MS/MS Deconvolution for Comprehensive Metabolome Analysis. *Nat. Methods* **2015**, *12* (6), 523−526.
(30) Chong, J.; Yamamoto, M.; Xia, J. MetaboAnalystR 2.0: From Raw Spectra to Biological Insights. *Metabolites* **2019**, *9* (3), 57.
(31) Kirk, R. D.; He, H.; Wahome, P. G.; Wu, S.; Carter, G. T.; Bertin, M. J. New micropeptins with anti-neuroinflammatory activity isolated from a cyanobacterial bloom. *ACS Omega* **2021**, *6*, 15472−15478.
(32) Wu, Y.; Li, L.; Zheng, L.; Dai, G.; Ma, H.; Shan, K.; Wu, H.; Zhou, Q.; Song, L. Patterns of Succession between Bloom-Forming Cyanobacteria *Aphanizomenon flos-aquae* and *Microcystis* and Related Environmental Factors in Large, Shallow Dianchi Lake, China. *Hydrobiologia* **2016**, *765* (1), 1−13.
(33) Shan, K.; Song, L.; Chen, W.; Li, L.; Liu, L.; Wu, Y.; Jia, Y.; Zhou, Q.; Peng, L. Analysis of Environmental Drivers Influencing Interspecific Variations and Associations among Bloom-Forming Cyanobacteria in Large, Shallow Eutrophic Lakes. *Harmful Algae* **2019**, *84*, 84−94.
(34) Paerl, H. W.; Hall, N. S.; Calandrino, E. S. Controlling Harmful Cyanobacterial Blooms in a World Experiencing Anthropogenic and Climatic-Induced Change. *Sci. Total Environ.* **2011**, *409* (10), 1739−1745.
(35) Kosten, S.; Huszar, V. L. M.; Bécares, E.; Costa, L. S.; van Donk, E.; Hansson, L.-A.; Jeppesen, E.; Kruk, C.; Lacerot, G.; Mazzeo, N.; de Meester, L.; Moss, B.; Lürling, M.; Nõges, T.; Romo, S.; Scheffer, M. Warmer Climates Boost Cyanobacterial Dominance in Shallow Lakes. *Global Change Biol.* **2012**, *18*, 118−126.
(36) Barnard, M. A.; Chaffin, J. D.; Plaas, H. E.; Boyer, G. L.; Wei, B.; Wilhelm, S. W.; Rossignol, K. L.; Braddy, J. S.; Bullerjahn, G. S.; Bridgeman, T. B.; Davis, T. W.; Wei, J.; Bu, M.; Paerl, H. W. Roles of Nutrient Limitation on Western Lake Erie CyanoHAB Toxin Production. *Toxins* **2021**, *13* (1), 47.
(37) Gobler, C. J.; Burkholder, J. M.; Davis, T. W.; Harke, M. J.; Johengen, T.; Stow, C. A.; Van de Waal, D. B. The Dual Role of Nitrogen Supply in Controlling the Growth and Toxicity of Cyanobacterial Blooms. *Harmful Algae* **2016**, *54*, 87−97.

https://doi.org/10.1021/acsestwater.4c00266
ACS EST Water 2024, 4, 3423−3432

(38) Pimentel, J. S.; Giani, A. Microcystin Production and Regulation under Nutrient Stress Conditions in Toxic *Microcystis* Strains. *Appl. Environ. Microbiol.* **2014**, *80* (18), 5836−5843.
(39) Berg, K. A.; Lyra, C.; Sivonen, K.; Paulin, L.; Suomalainen, S.; Tuomi, P.; Rapala, J. High Diversity of Cultivable Heterotrophic Bacteria in Association with Cyanobacterial Water Blooms. *ISME J.* **2009**, *3* (3), 314−325.
(40) Zastepa, A.; Westrick, J. A.; Liang, A.; Birbeck, J. A.; Furr, E.; Watson, L. C.; Stockdill, J. L.; Ramakrishna, B. S.; Crevecoeur, S. Broad Screening of Toxic and Bioactive Metabolites in Cyanobacterial and Harmful Algal Blooms in Lake of the Woods (Canada and USA), 2016−2019. *J. Great Lakes Res.* **2023**, *49* (1), 134−146.
(41) Rolland, D. C.; Bourget, S.; Warren, A.; Laurion, I.; Vincent, W. F. Extreme Variability of Cyanobacterial Blooms in an Urban Drinking Water Supply. *J. Plankton Res.* **2013**, *35* (4), 744−758.
(42) Dreher, T. W.; Matthews, R.; Davis, E. W.; Mueller, R. S. *Woronichinia naegeliana*: A Common Nontoxigenic Component of Temperate Freshwater Cyanobacterial Blooms with 30% of Its Genome in Transposons. *Harmful Algae* **2023**, *125*, 102433.
(43) Bober, B.; Bialczyk, J. Determination of the Toxicity of the Freshwater Cyanobacterium *Woronichinia naegeliana* (Unger) Elenkin. *J. Appl. Phycol.* **2017**, *29* (3), 1355−1362.
(44) Kim Tiam, S.; Gugger, M.; Demay, J.; Le Manach, S.; Duval, C.; Bernard, C.; Marie, B. Insights into the Diversity of Secondary Metabolites of Planktothrix Using a Biphasic Approach Combining Global Genomics and Metabolomics. *Toxins* **2019**, *11* (9), 498.
(45) Le Manach, S.; Duval, C.; Marie, A.; Djediat, C.; Catherine, A.; Edery, M.; Bernard, C.; Marie, B. Global Metabolomic Characterizations of *Microcystis* spp. Highlights Clonal Diversity in Natural Bloom-Forming Populations and Expands Metabolite Structural Diversity. *Front. Microbiol.* **2019**, *10*, 791.
(46) Kust, A.; Řeháková, K.; Vrba, J.; Maicher, V.; Mareš, J.; Hrouzek, P.; Chiriac, M.-C.; Benedová, Z.; Tesařová, B.; Saurav, K. Insight into Unprecedented Diversity of Cyanopeptides in Eutrophic Ponds Using an MS/MS Networking Approach. *Toxins* **2020**, *12* (9), 561.
(47) McDonald, K.; DesRochers, N.; Renaud, J. B.; Sumarah, M. W.; McMullin, D. R. Metabolomics Reveals Strain-Specific Cyanopeptide Profiles and Their Production Dynamics in *Microcystis aeruginosa* and *M. flos-aquae*. *Toxins* **2023**, *15* (4), 254.
(48) Teta, R.; Della Sala, G.; Glukhov, E.; Gerwick, L.; Gerwick, W. H.; Mangoni, A.; Costantino, V. Combined LC−MS/MS and Molecular Networking Approach Reveals New Cyanotoxins from the 2014 Cyanobacterial Bloom in Green Lake, Seattle. *Environ. Sci. Technol.* **2015**, *49* (24), 14301−14310.
(49) Tang, X.; Krausfeldt, L. E.; Shao, K.; LeCleir, G. R.; Stough, J. M. A.; Gao, G.; Boyer, G. L.; Zhang, Y.; Paerl, H. W.; Qin, B.; Wilhelm, S. W. Seasonal Gene Expression and the Ecophysiological Implications of Toxic *Microcystis aeruginosa* Blooms in Lake Taihu. *Environ. Sci. Technol.* **2018**, *52* (19), 11049−11059.
(50) Li, H.; Bhattarai, B.; Barber, M.; Goel, R. Stringent Response of Cyanobacteria and Other Bacterioplankton during Different Stages of a Harmful Cyanobacterial Bloom. *Environ. Sci. Technol.* **2023**, *57* (42), 16016−16032.
(51) Humphrey, J. M.; Aggen, J. B.; Chamberlin, A. R. Total Synthesis of the Serine-Threonine Phosphatase Inhibitor Microcystin-LA. *J. Am. Chem. Soc.* **1996**, *118* (47), 11759−11770.
(52) Liang, S.; Xu, Z.; Ye, T. Total Synthesis of Largamide H. *Chem. Commun.* **2010**, *46*, 153−155.
(53) Sivonen, K.; Skulberg, O. M.; Namikoshi, M.; Evans, W. R.; Carmichael, W. W.; Rinehart, K. L. Two Methyl Ester Derivatives of Microcystins, Cyclic Heptapeptide Hepatotoxins, Isolated from *Anabaena flos-aquae* Strain CYA 83/1. *Toxicon* **1992**, *30* (11), 1465−1471.
(54) Teta, R.; Della Sala, G.; Glukhov, E.; Gerwick, L.; Gerwick, W. H.; Mangoni, A.; Costantino, V. Combined LC−MS/MS and Molecular Networking Approach Reveals New Cyanotoxins from the 2014 Cyanobacterial Bloom in Green Lake, Seattle. *Environ. Sci. Technol.* **2015**, *49*, 14301−14310.
(55) Mallia, V.; Uhlig, S.; Rafuse, C.; Meija, J.; Miles, C. O. Novel Microcystins from *Planktothrix prolifica* NIVA-CYA 544 Identified by LC-MS/MS, Functional Group Derivatization and ^{15}N-labeling. *Mar. Drugs* **2019**, *17* (11), 643.
(56) (a) Wen, Q.; Xiao, P.; Li, H.; Li, W.; Yu, G.; Li, R. Succession of Aphanizomenon flos-aquae and Microcystis aeruginosa in Direct Co-Culture Experiments at Different Temperatures and Biomasses. *J. Oceanol. Limnol.* **2022**, *40* (5), 1819−1828. (b) Duperron, S.; Halary, S.; Habiballah, M.; Gallet, A.; Huet, H.; Duval, C.; Bernard, C.; Marie, B. Response of Fish Gut Microbiota to Toxin-Containing Cyanobacterial Extracts: A Microcosm Study on the Medaka (Oryzias latipes). *Environ. Sci. Technol. Lett.* **2019**, *6* (6), 341−347.
(57) Torres, M. D. A.; Jones, M. R.; vom Berg, C.; Pinto, E.; Janssen, E. M.-L. Lethal and Sublethal Effects towards Zebrafish Larvae of Microcystins and Other Cyanopeptides Produced by Cyanobacteria. *Aquat. Toxicol.* **2023**, *263*, 106689.
(58) Marrone, B. L.; Banerjee, S.; Talapatra, A.; Gonzalez-Esquer, C. R.; Pilania, G. Toward a Predictive Understanding of Cyanobacterial Harmful Algal Blooms through AI Integration of Physical, Chemical, and Biological Data. *ACS EST Water* **2024**, *4* (3), 844−858.

https://doi.org/10.1021/acsestwater.4c00266
ACS EST Water 2024, 4, 3423−3432